



Spin-dependent part of $\bar{p}d$ interaction cross section and Nijmegen potential

S.G. Salnikov

Budker Institute of Nuclear Physics, 630090 Novosibirsk, Russia

Received 14 September 2011; received in revised form 16 November 2011; accepted 18 November 2011

Available online 22 November 2011

Abstract

Low energy $\bar{p}d$ interaction is considered taking into account the polarization of both particles. The corresponding cross sections are obtained using the Nijmegen nucleon–antinucleon optical potential with shadowing effects taken into account. Double-scattering effects are calculated within the Glauber approach and found to be about 10–20%. The cross sections are applied to the analysis of the polarization buildup which is due to the interaction of stored antiprotons with a polarized target. It is shown that, at realistic parameters of a storage ring and a target, the filtering mechanism may provide a noticeable polarization in a time comparable with the beam lifetime. The energy dependence of the polarization rate for deuterium target is similar to that for hydrogen one. However, the time of polarization for deuterium is much smaller than that for hydrogen.

© 2011 Elsevier B.V. All rights reserved.

Keywords: Polarization; Antiprotons; Nijmegen; Glauber; Deuteron

1. Introduction

An extensive research program with polarized antiprotons has been proposed recently by the PAX Collaboration [1]. This program initiated a discussion of various methods to polarize stored antiprotons. One of the methods being considered is to use multiple scattering off a polarized target. If all particles remain in the beam (scattering angle is smaller than the acceptance angle θ_{acc}), only spin flip can lead to polarization buildup, as was shown in Refs. [2,3]. However, spin-flip cross section is negligibly small [2,4]. Hence the most realistic method is spin filtering [5]. This method implements the dependence of the cross section on orientation of the spins of the

E-mail address: salsergey@gmail.com.

particles. Therefore the number of antiprotons scattered out of the beam after the interaction with a polarized target depends on their spins, which results in the polarization buildup. The interaction with atomic electrons can't provide noticeable polarization because in this case antiprotons will scatter only in small angles and all antiprotons remain in the beam [2]. Thus it is necessary to study antiproton–nuclear scattering.

At present, theory can't give reliable predictions for $\bar{p}N$ cross section below 1 GeV and different phenomenological models are usually used for numerical estimations. As a result, the cross sections obtained are model-dependent. All models are based on fitting experimental data for scattering of unpolarized particles. These models give similar predictions for spin-independent part of the cross sections, but predictions for spin-dependent parts may differ drastically.

Different nucleon–antinucleon potentials have similar behavior at large distance ($r \gtrsim 1$ fm) because long-range potentials are obtained by applying G-parity transformation to well-known nucleon–nucleon potential. The most important difference between nucleon–antinucleon and nucleon–nucleon scattering is existence of annihilation channels. A phenomenological description of annihilation is usually based on an optical potential of the form

$$V_{N\bar{N}} = U_{N\bar{N}} - iW_{N\bar{N}}. \quad (1)$$

Imaginary part of this potential describes annihilation into mesons and is important at small distance. The process of annihilation has no generally accepted description, and short-range potentials in various models are different.

One of the methods to polarize antiprotons being investigated is to use scattering off a polarized hydrogen target. Spin-dependent parts of the cross section of $\bar{p}p$ interaction were previously calculated in Ref. [6] using the Paris potential and in Ref. [7] with the help of the Nijmegen potential. Similar calculations were performed in Ref. [8] where various forms of Julich potentials were explored. All models listed above predict a possibility to obtain a noticeable beam polarization in a reasonable time, but the value of the polarization degree predicted is essentially different.

Another possibility to polarize stored antiprotons being considered is to use polarized deuteron target instead of a hydrogen target. Theoretical investigation of antiproton–deuteron scattering is the subject present paper is devoted to. We make use of the Nijmegen model to calculate $\bar{p}N$ scattering amplitudes. In order to calculate $\bar{p}d$ cross sections we utilize the Glauber theory [9,10]. We believe that the Glauber approach has sufficient precision for the description of $\bar{p}d$ scattering in the energy region concerned. The figures confirming this statement are presented in Section 3. In the present paper we show the predictions for the spin-dependent parts of $\bar{p}d$ cross sections based on the Nijmegen model along with the expected antiproton beam polarization degree. The comparison with the predictions from Ref. [11] based on the Julich models is also considered in this paper.

2. Method of calculation

Our method of calculation is similar to that described in Ref. [11]. We make use of the Glauber theory to describe scattering by a deuteron. In the present paper we give the formulas for the standard Glauber theory [9] which doesn't include the D-wave contribution in the deuteron wave function and the spin dependence of $\bar{p}N$ scattering amplitudes. The modification of this theory taking these factors into account for the case of pd scattering can be found in Ref. [12]. Within the standard Glauber theory the amplitudes for elastic and breakup scattering are given by the following matrix elements

$$F_{fi}^{\bar{p}d}(\mathbf{q}) = \langle f | F^{\bar{p}d}(\mathbf{q}, \mathbf{s}) | i \rangle \quad (2)$$

between initial $|i\rangle$ and final $|f\rangle$ states of the two-nucleon system. Here the transition operator is

$$F^{\bar{p}d}(\mathbf{q}, \mathbf{s}) = e^{\frac{1}{2}i\mathbf{q}\cdot\mathbf{s}} f_{\bar{p}p}(\mathbf{q}) + e^{-\frac{1}{2}i\mathbf{q}\cdot\mathbf{s}} f_{\bar{p}n}(\mathbf{q}) \\ + \frac{i}{2\pi k_{\bar{p}d}} \int e^{i\mathbf{q}'\cdot\mathbf{s}} f_{\bar{p}p}\left(\frac{1}{2}\mathbf{q} - \mathbf{q}'\right) f_{\bar{p}n}\left(\frac{1}{2}\mathbf{q} + \mathbf{q}'\right) d^2\mathbf{q}', \quad (3)$$

where \mathbf{q} is the momentum transfer, \mathbf{s} is the impact parameter (the transverse component of \mathbf{r}), $f_{\bar{p}N}(\mathbf{q})$ are antiproton–nucleon elastic scattering amplitudes and $k_{\bar{p}d} = \sqrt{m_N T_{\text{lab}}}/2$ is the antiproton momentum, m_N being the nucleon mass and T_{lab} being the antiproton kinetic energy in the laboratory frame. Note that the antiproton momentum and antiproton–nucleon scattering amplitudes should be calculated in the same reference system. Using Eqs. (2) and (3) one obtains the following equation for the elastic antiproton–deuteron scattering amplitude:

$$F_{ii}^{\bar{p}d}(\mathbf{q}) = S\left(\frac{\mathbf{q}}{2}\right) f_{\bar{p}p}(\mathbf{q}) + S\left(-\frac{\mathbf{q}}{2}\right) f_{\bar{p}n}(\mathbf{q}) \\ + \frac{i}{2\pi k_{\bar{p}d}} \int S(\mathbf{q}') f_{\bar{p}p}\left(\frac{1}{2}\mathbf{q} - \mathbf{q}'\right) f_{\bar{p}n}\left(\frac{1}{2}\mathbf{q} + \mathbf{q}'\right) d^2\mathbf{q}'. \quad (4)$$

Note that the latter formula involves only the elastic deuteron form factor $S(\mathbf{q})$ and amplitudes of $\bar{p}N$ scattering. Elastic ($\bar{p}d \rightarrow \bar{p}d$) differential cross section is given by

$$\left(\frac{d\sigma}{d\Omega}\right)_{\text{el}} = |F_{ii}^{\bar{p}d}(\mathbf{q})|^2. \quad (5)$$

If one neglects the energy difference of various final states then the sum of elastic plus inelastic ($\bar{p}d \rightarrow \bar{p}pn$) cross sections can be calculated in the following way:

$$\left(\frac{d\sigma}{d\Omega}\right)_{\text{sc}} = \sum_f |F_{fi}^{\bar{p}d}(\mathbf{q})|^2 = \langle i | |F^{\bar{p}d}(\mathbf{q}, \mathbf{s})|^2 | i \rangle = |f_{\bar{p}p}(\mathbf{q})|^2 + |f_{\bar{p}n}(\mathbf{q})|^2 \\ + 2S(\mathbf{q}) \text{Re}[f_{\bar{p}n}(\mathbf{q}) f_{\bar{p}p}^*(\mathbf{q})] \\ - \frac{1}{\pi k_{\bar{p}d}} \text{Im} \left[f_{\bar{p}n}^*(\mathbf{q}) \int S\left(\mathbf{q}' - \frac{1}{2}\mathbf{q}\right) f_{\bar{p}p}\left(\frac{1}{2}\mathbf{q} - \mathbf{q}'\right) f_{\bar{p}n}\left(\frac{1}{2}\mathbf{q} + \mathbf{q}'\right) d^2\mathbf{q}' \right] \\ - \frac{1}{\pi k_{\bar{p}d}} \text{Im} \left[f_{\bar{p}p}^*(\mathbf{q}) \int S\left(\mathbf{q}' + \frac{1}{2}\mathbf{q}\right) f_{\bar{p}p}\left(\frac{1}{2}\mathbf{q} - \mathbf{q}'\right) f_{\bar{p}n}\left(\frac{1}{2}\mathbf{q} + \mathbf{q}'\right) d^2\mathbf{q}' \right] \\ + \frac{1}{(2\pi k_{\bar{p}d})^2} \int d^3\mathbf{r} |\phi(\mathbf{r})|^2 \left| \int e^{i\mathbf{q}'\cdot\mathbf{s}} f_{\bar{p}p}\left(\frac{1}{2}\mathbf{q} - \mathbf{q}'\right) f_{\bar{p}n}\left(\frac{1}{2}\mathbf{q} + \mathbf{q}'\right) d^2\mathbf{q}' \right|^2. \quad (6)$$

The amplitudes of antinucleon–nucleon scattering were calculated with the help of the Nijmegen antinucleon–nucleon optical potential [13] in the same way as in our previous work [7].

The total spin-dependent $\bar{p}d$ cross section can be written in the form [11]

$$\sigma = \sigma_0 + \sigma_1(\mathbf{P}^{\bar{p}} \cdot \mathbf{P}^d) + (\sigma_2 - \sigma_1)(\mathbf{P}^{\bar{p}} \cdot \mathbf{v})(\mathbf{P}^d \cdot \mathbf{v}) + \sigma_3 P_{zz}^d, \quad (7)$$

where \mathbf{P}^i are the polarization vectors of corresponding particles, P_{zz}^d is the component of the deuteron tensor polarization and \mathbf{v} is the unit momentum vector. The cross section σ_3 vanishes in the single-scattering approximation [11]. This cross section turned out to be much smaller

than the cross sections σ_1 and σ_2 . This statement is valid also if the shadowing effects are taken into account. The cross section σ_3 has no influence on the antiproton polarization and we neglect this cross section in our further calculations. Spin-dependent parts of the cross section can be expressed in terms of the scattering amplitudes g_i in the following way [11]

$$\begin{aligned}\sigma_0 &= \frac{2\pi}{k_{\bar{p}d}} \text{Im}(g_1 + g_2), & \sigma_1 &= \frac{4\pi}{k_{\bar{p}d}} \text{Im} g_3, \\ \sigma_2 &= \frac{4\pi}{k_{\bar{p}d}} \text{Im} g_4, & \sigma_3 &= \frac{4\pi}{k_{\bar{p}d}} \text{Im} \frac{g_1 - g_2}{6}.\end{aligned}\quad (8)$$

Here

$$\begin{aligned}g_1 &= \frac{1}{2} \left(\left\langle +\frac{1}{2}, -1 \left| F^{\bar{p}d}(0) \right| +\frac{1}{2}, -1 \right\rangle + \left\langle +\frac{1}{2}, +1 \left| F^{\bar{p}d}(0) \right| +\frac{1}{2}, +1 \right\rangle \right), \\ g_2 &= \left\langle +\frac{1}{2}, 0 \left| F^{\bar{p}d}(0) \right| +\frac{1}{2}, 0 \right\rangle, \\ g_3 &= -\frac{1}{\sqrt{2}} \left\langle +\frac{1}{2}, -1 \left| F^{\bar{p}d}(0) \right| -\frac{1}{2}, 0 \right\rangle, \\ g_4 &= \frac{1}{2} \left(\left\langle +\frac{1}{2}, -1 \left| F^{\bar{p}d}(0) \right| +\frac{1}{2}, -1 \right\rangle - \left\langle +\frac{1}{2}, +1 \left| F^{\bar{p}d}(0) \right| +\frac{1}{2}, +1 \right\rangle \right).\end{aligned}\quad (9)$$

In order to calculate these amplitudes we have substituted Eq. (4) in the latter equations. One can see that it is necessary to calculate the matrix elements of antiproton–nucleon scattering operators between deuteron states with definite spin projections. A convenient way to perform such calculations is to express the deuteron spin wave functions via the proton and neutron spin wave functions. For instance,

$$\begin{aligned}& \left\langle \frac{1}{2}, 1 \left| F^{\bar{p}d}(0) \right| \frac{1}{2}, 1 \right\rangle \\ &= S(0) \left\langle \frac{1}{2}, \frac{1}{2} \left| f_{\bar{p}p}(0) \right| \frac{1}{2}, \frac{1}{2} \right\rangle + S(0) \left\langle \frac{1}{2}, \frac{1}{2} \left| f_{\bar{p}n}(0) \right| \frac{1}{2}, \frac{1}{2} \right\rangle \\ &+ \frac{i}{2\pi k_{\bar{p}d}} \int S(\mathbf{q}') \sum_{\lambda} \left\langle \frac{1}{2}, \frac{1}{2} \left| f_{\bar{p}p}(-\mathbf{q}') \right| \lambda, \frac{1}{2} \right\rangle \left\langle \lambda, \frac{1}{2} \left| f_{\bar{p}n}(\mathbf{q}') \right| \frac{1}{2}, \frac{1}{2} \right\rangle d^2\mathbf{q}',\end{aligned}\quad (10)$$

where λ is the intermediate antiproton spin. The scattering amplitudes with other projections of antiproton and deuteron spins have similar form.

It was shown that the interference of the Coulomb and nuclear amplitudes is important for the description of the spin-dependent parts of the $\bar{p}p$ cross section (see f.i. Refs. [6,7]). One can expect that interference is also important for the description of $\bar{p}d$ cross section. The formulas for the contribution of interference to unpolarized and polarized cross sections of $\bar{p}d$ scattering are taken from Ref. [11]. In terms of the amplitudes g_i , they are

$$\begin{aligned}\sigma_0^{\text{int}} &= -\frac{2\pi}{k_{\bar{p}p}} \left\{ \cos 2\chi_0 \left[-\sin \Psi \text{Re}(g_1 + g_2) + (1 - \cos \Psi) \text{Im}(g_1 + g_2) \right] \right. \\ &\quad \left. - \sin 2\chi_0 \left[\sin \Psi \text{Im}(g_1 + g_2) + (1 - \cos \Psi) \text{Re}(g_1 + g_2) \right] \right\}, \\ \sigma_1^{\text{int}} &= -\frac{4\pi}{k_{\bar{p}p}} \left\{ \cos 2\chi_0 \left[-\sin \Psi \text{Re} g_3 + (1 - \cos \Psi) \text{Im} g_3 \right] \right\}\end{aligned}$$

$$\begin{aligned} & -\sin 2\chi_0[\sin \Psi \operatorname{Im} g_3 + (1 - \cos \Psi) \operatorname{Re} g_3] \}, \\ \sigma_2^{\text{int}} = & -\frac{4\pi}{k_{\bar{p}p}} \{ \cos 2\chi_0[-\sin \Psi \operatorname{Re} g_4 + (1 - \cos \Psi) \operatorname{Im} g_4] \\ & + \sin 2\chi_0[\sin \Psi \operatorname{Im} g_4 - (1 - \cos \Psi) \operatorname{Re} g_4] \}, \end{aligned} \quad (11)$$

where $\Psi = -\frac{\alpha}{v} \ln \sin \theta_{\text{acc}}/2$, $\chi_0 = \arg \Gamma(1 - \frac{i\alpha}{2v})$ is the Coulomb phase, α is the fine structure constant and v is the velocity of the antiproton in the $\bar{p}p$ center-of-mass frame. For the pure Coulomb interaction the cross sections σ_1 , σ_2 are zero and σ_0 is

$$\sigma_0^{\text{C}} = \frac{\pi \alpha^2}{(vk_{\bar{p}p}\theta_{\text{acc}})^2}, \quad (12)$$

where $k_{\bar{p}p}$ is the antiproton momentum in the $\bar{p}p$ center-of-mass frame and smallness of θ_{acc} is taken into account.

One can find the discussion of antiproton beam polarization buildup in Refs. [2,6]. Shown here is only the final result for the polarization degree at time $t_0 = 2\tau_b$, $\tau_b = 1/nf\sigma_0$ being the beam lifetime subject to scattering by the target:

$$P_B(t_0) = \begin{cases} -2P_T \frac{\sigma_1}{\sigma_0}, & \text{if } \boldsymbol{\zeta}_T \cdot \mathbf{v} = 0, \\ -2P_T \frac{\sigma_2}{\sigma_0}, & \text{if } |\boldsymbol{\zeta}_T \cdot \mathbf{v}| = 1. \end{cases} \quad (13)$$

Here \mathbf{v} is the unit vector collinear to the antiproton momentum, $\boldsymbol{\zeta}_T$ is the direction of the target polarization, P_T is the value of the target polarization, n is the areal density of the target and f is the beam revolving frequency. The equalities (13) are valid in both cases $\boldsymbol{\zeta}_T \perp \mathbf{v}$ and $\boldsymbol{\zeta}_T \parallel \mathbf{v}$.

3. Results

In this section we present numerical results for the spin-dependent parts of the cross sections of $\bar{p}p$, $\bar{p}n$ and $\bar{p}d$ scattering along with the predictions for the beam polarization degree obtained with the help of the Nijmegen model [13]. The results for total unpolarized $\bar{p}p$ and $\bar{p}n$ cross sections are in good agreement with all available experimental data. Unpolarized cross sections were studied both theoretically and experimentally by many authors so there is no necessity to present the corresponding figures here. However, the situation is different for the spin-dependent parts of the cross sections because they were not studied experimentally and different theoretical models provide essentially different predictions. The predictions of the Nijmegen model for the spin-dependent parts of $\bar{p}p$ cross section were previously presented in Ref. [7], but we show them here for completeness. The dependence of the spin-dependent parts of the cross section of $\bar{p}p$ and $\bar{p}n$ scattering on the antiproton energy is shown in Fig. 1. One can see that σ_2 is of the same order for these two processes, but σ_1 for $\bar{p}n$ scattering is smaller than that for $\bar{p}p$ scattering. Note that the sign of the interference contribution to $\bar{p}n$ scattering differs from that to $\bar{p}p$ scattering. It results in smaller interference contribution to $\bar{p}d$ scattering.

In order to estimate the role of double-scattering mechanism in $\bar{p}d$ scattering we have calculated the total unpolarized $\bar{p}d$ cross section, see Fig. 2(a). One can see that the shadowing effects decrease the total cross section at about 15% in the whole energy region and that was the case for the Julich potential too, see Ref. [11]. The line obtained in the current work approximates the experimental data [15–19] quite accurately.

We also present here the differential elastic ($\bar{p}d \rightarrow \bar{p}d$) and elastic plus inelastic ($\bar{p}d \rightarrow \bar{p}pn$) cross sections, see Fig. 3. These quantities are interesting for us because the double-scattering

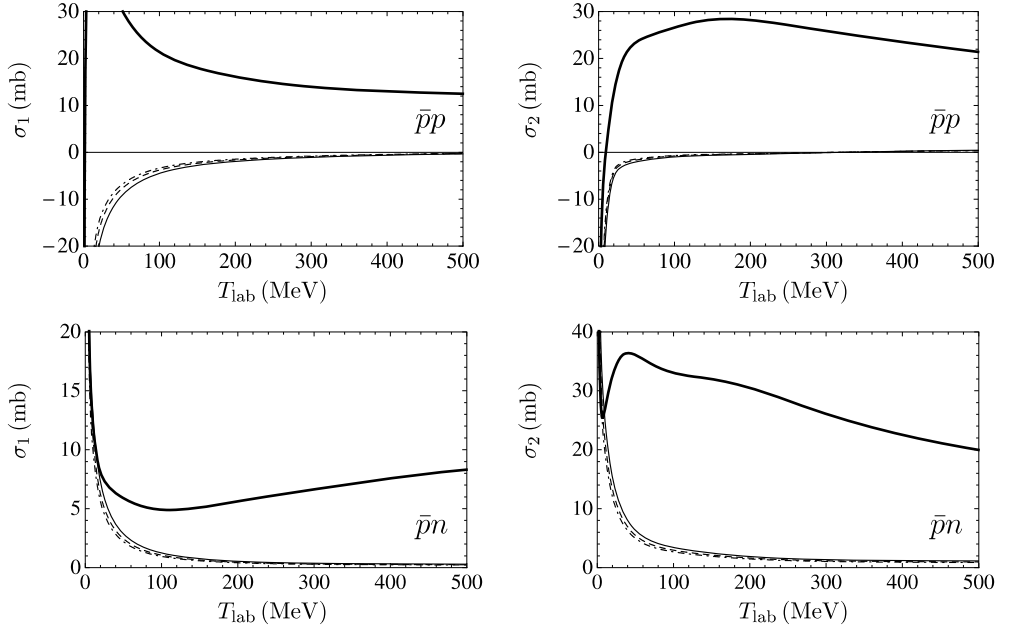


Fig. 1. The dependence of hadronic cross sections σ_1^h , σ_2^h (thick line) and the Coulomb-hadronic interference contributions σ_1^{int} , σ_2^{int} (thin lines) on T_{lab} for $\bar{p}p$ scattering (upper row) and $\bar{p}n$ scattering (lower row). The interference contribution in the lower row is the interference of the Coulomb $\bar{p}p$ and strong $\bar{p}n$ amplitudes for $\bar{p}d$ scattering. The acceptance angles in the lab frame are $\theta_{\text{acc}}^{(l)} = 10$ mrad (solid line), $\theta_{\text{acc}}^{(l)} = 20$ mrad (dashed line), $\theta_{\text{acc}}^{(l)} = 30$ mrad (dashed-dotted line).

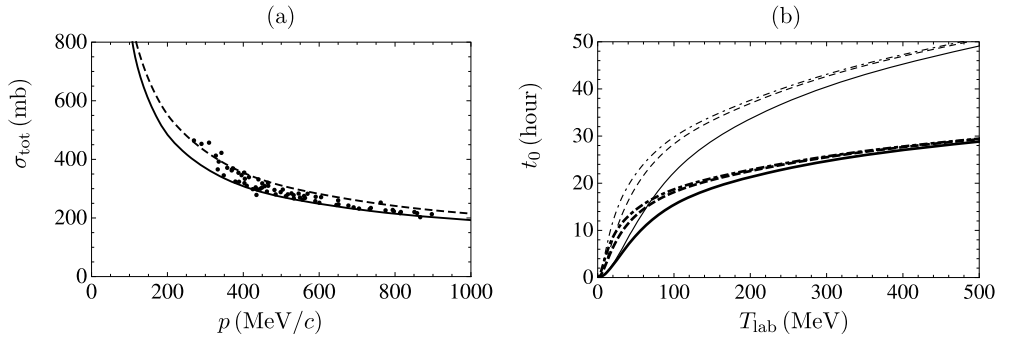


Fig. 2. (a) The dependence of the total $\bar{p}d$ cross section on p_{lab} within the single-scattering approximation (dashed line) and including shadowing effects (solid line). Data are taken from Refs. [15–19]. (b) The dependence of the polarization time t_0 on T_{lab} for $n = 10^{14} \text{ cm}^{-2}$ and $f = 10^6 \text{ c}^{-1}$ for $\bar{p}d$ scattering (thick lines) and $\bar{p}p$ scattering (thin lines). The acceptance angles in the lab frame are $\theta_{\text{acc}}^{(l)} = 10$ mrad (solid line), $\theta_{\text{acc}}^{(l)} = 20$ mrad (dashed line), $\theta_{\text{acc}}^{(l)} = 30$ mrad (dashed-dotted line).

mechanism is very important for accurate description of non-forward $\bar{p}d$ scattering and we can test the applicability of the Glauber theory to low-energy $\bar{p}d$ scattering comparing our results with the existing experimental data. We have included the D-wave contribution with the method described in Ref. [10] while calculating the elastic differential cross sections. In order to calculate

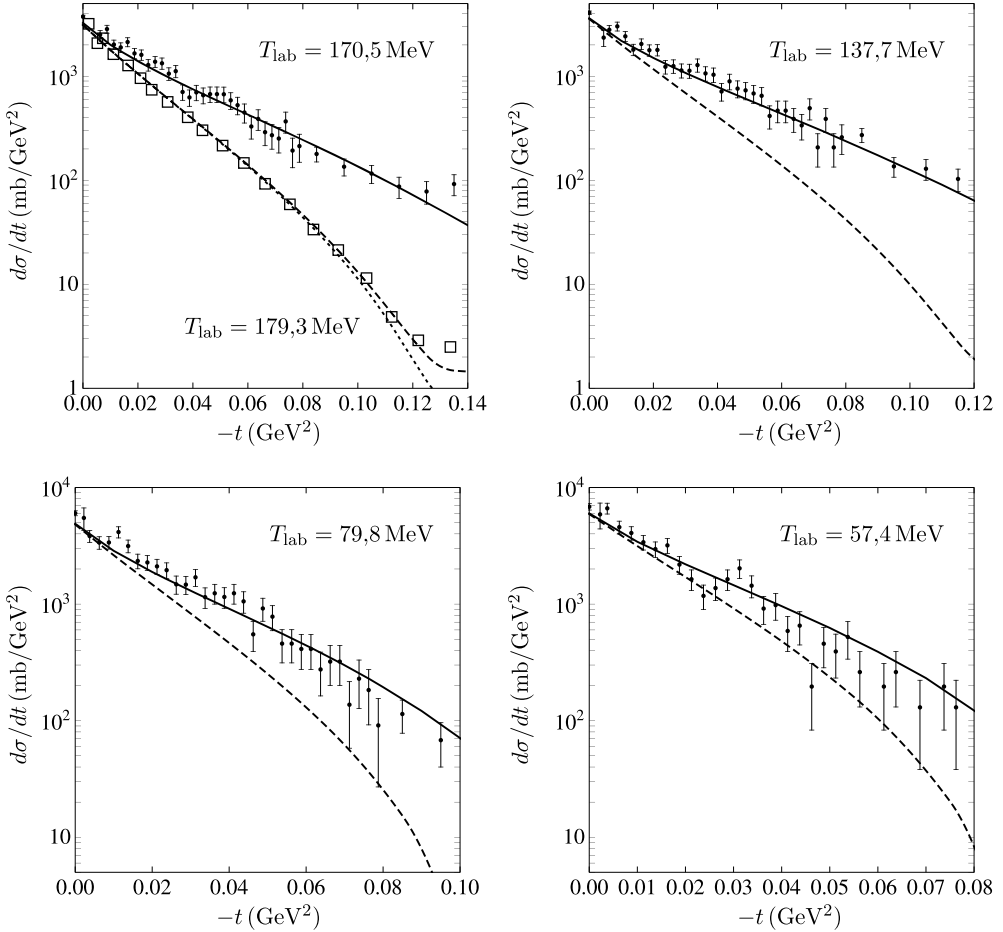


Fig. 3. The dependence of elastic (dashed lines) and elastic plus inelastic (solid lines) $\bar{p}d$ differential cross sections on the momentum transfer. Dotted line for $T_{\text{lab}} = 179.3$ MeV corresponds to the cross section calculated without the inclusion of the D-wave contribution. Data for the elastic scattering cross section (squares) are taken from Ref. [20] and for elastic plus inelastic cross sections (dots) from Ref. [15].

the two form-factors needed by the theory, the numerical values for the deuteron wave function calculated in Ref. [14] using the Paris model were used. In order to estimate the role of the D-wave contribution we present the cross section without D-wave being included in the same figure. As we expected, the D-wave contribution proved to be significant only for scattering with large momentum transfer because the corresponding form-factor vanishes in the case of forward scattering. Experimental data for the elastic $\bar{p}d$ scattering exist only at 180 MeV [20] (squares in Fig. 3) and are nicely reproduced by our line. Experimental data for elastic plus inelastic scattering [15] are also reproduced quite well, see Fig. 3. The Glauber theory seems to be applicable for the description of unpolarized $\bar{p}d$ cross sections at rather low energies down to 50 MeV.

The spin-dependent parts of the cross section of $\bar{p}d$ scattering were calculated with the double-scattering mechanism taken into account. However, the contribution of D-wave in the

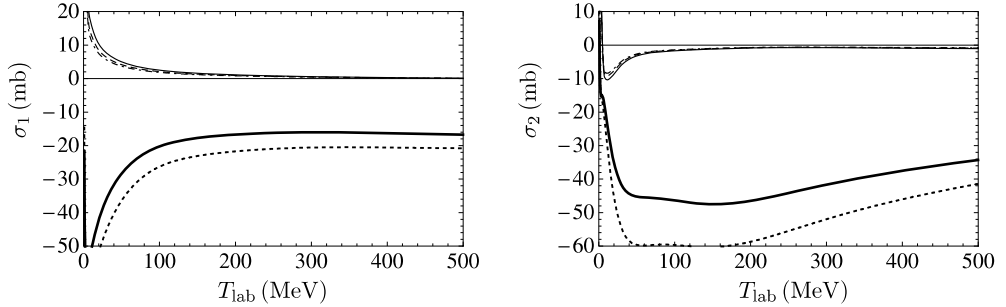


Fig. 4. The dependence of σ_1 , σ_2 (thick line) and interference contributions σ_1^{int} , σ_2^{int} (thin lines) on T_{lab} for $\bar{p}d$ scattering. Lower dotted line corresponds to the cross section calculated in the single-scattering approximation. The acceptance angles in the lab frame are $\theta_{\text{acc}}^{(l)} = 10$ mrad (solid line), $\theta_{\text{acc}}^{(l)} = 20$ mrad (dashed line), $\theta_{\text{acc}}^{(l)} = 30$ mrad (dashed-dotted line).

deuteron wave function was omitted because we expect it to be less important. The spin-dependent parts of $\bar{p}d$ cross section are presented in Fig. 4. The interference contribution to $\bar{p}d$ cross section proved to be less significant in most part of the energy range than it was for $\bar{p}p$ scattering. The validity of this conclusion for the Julich model was previously shown in Ref. [11]. Shadowing effects turned out to decrease the absolute value of the cross sections σ_1 and σ_2 at about 20–25% level, see Fig. 4.

Let us proceed now to the discussion of the polarization buildup. The dependence of the time of polarization t_0 on the antiproton energy is presented in Fig. 2(b). Note that the number of antiprotons at time t_0 equals to 14% of the initial number. The dependence of transverse and longitudinal polarization degrees on the antiproton energy is shown in Fig. 5. Analogous results from Ref. [7] for $\bar{p}p$ scattering are also shown in that figure with the thin lines. One can see that the transverse polarization in the case of deuterium target is smaller than that in the case of hydrogen target. However, it is almost the same for energies below 50 MeV. The picture is different for longitudinal polarization. The longitudinal polarization degree in the case of $\bar{p}d$ scattering is larger for low energies, but it is almost the same as for $\bar{p}p$ scattering in most of energy range concerned.

It is important to note that theoretical predictions for the spin-dependent parts of $\bar{p}d$ cross section exhibit fairly strong model dependence. One can compare the predictions for the polarization degree following from the Nijmegen model with that from the Julich models, see Fig. 6. The predictions following from the Julich models are taken from Ref. [21]. Note that they are different from that in Ref. [11]. The polarization degree predicted by the Nijmegen model is about two or three times larger than that predicted by the Julich models and transverse polarization degree even has different sign.

4. Conclusion

We have calculated the cross section of antiproton–deuteron scattering making use of the Nijmegen nucleon–antinucleon potential and the Glauber theory for describing the scattering by a deuteron. The results obtained show the possibility to describe total and differential unpolarized $\bar{p}d$ cross sections in the whole energy region where the experimental data exist. The standard Glauber approach turned out to be sufficient for precise description of the scattering data with low momentum transfer. Taking into consideration the contribution of the spin-dependent parts

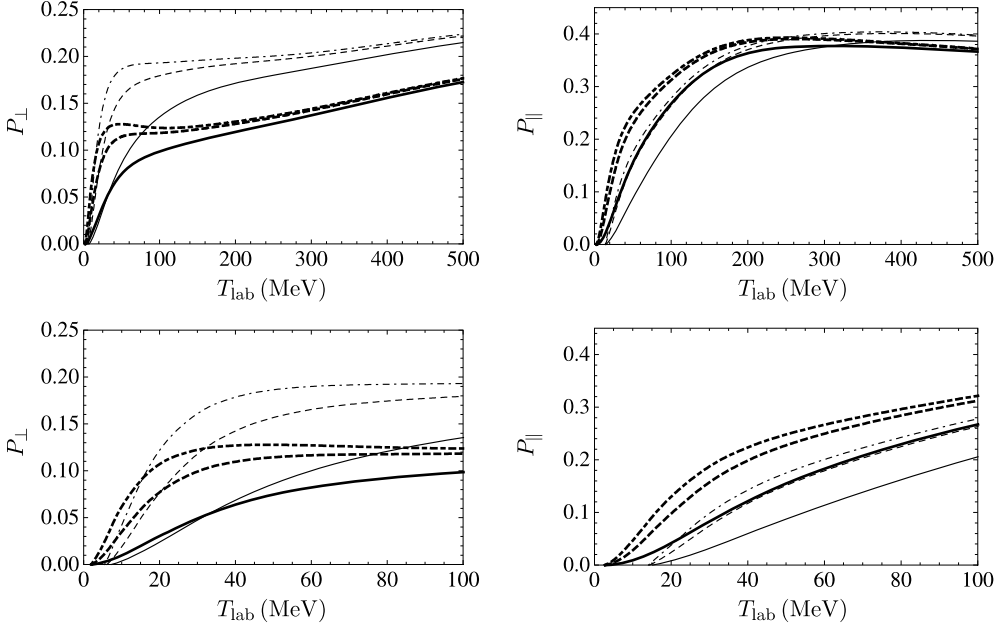


Fig. 5. The dependence of $P_B(t_0)$ for $P_T = 1$ on T_{lab} for $\zeta_T \cdot \mathbf{v} = 0$ (P_{\perp}) and $|\zeta_T \cdot \mathbf{v}| = 1$ (P_{\parallel}) for $\bar{p}d$ scattering (thick lines) in comparison with $\bar{p}p$ scattering (thin lines). Note that the polarization degree for $\bar{p}p$ scattering is shown with the opposite sign for simplicity. The acceptance angles in the lab frame are $\theta_{\text{acc}}^{(l)} = 10$ mrad (solid lines), $\theta_{\text{acc}}^{(l)} = 20$ mrad (dashed lines), $\theta_{\text{acc}}^{(l)} = 30$ mrad (dashed-dotted lines). Low energy region is shown again in the lower row.

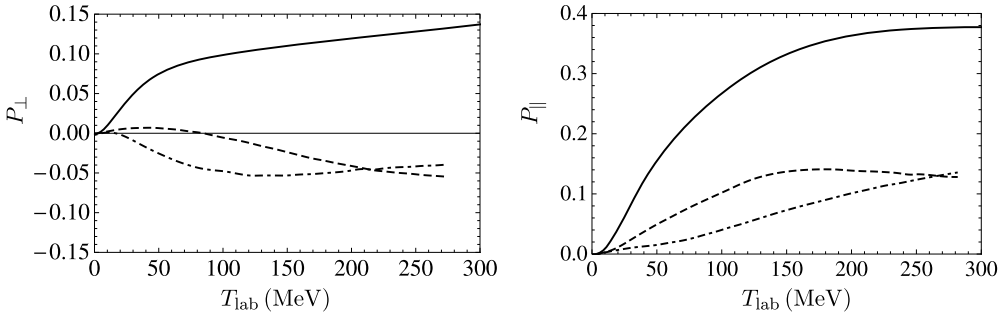


Fig. 6. The dependence of $P_B(t_0)$ for $P_T = 1$ on T_{lab} for $\zeta_T \cdot \mathbf{v} = 0$ (P_{\perp}) and $|\zeta_T \cdot \mathbf{v}| = 1$ (P_{\parallel}) for $\bar{p}d$ scattering for different models: Nijmegen model (solid line), Julich A model (dashed line) and Julich D model (dashed-dotted line). The acceptance angle in the lab frame is $\theta_{\text{acc}}^{(l)} = 10$ mrad.

of the nucleon–antinucleon amplitudes as well as D-wave part of the deuteron wave function to unpolarized $\bar{p}d$ cross section is important only for describing large-angle scattering. We confirm the conclusion about the applicability of the Glauber theory for the calculation of total and differential $\bar{p}d$ cross sections at rather low energies down to 50 MeV made in Refs. [11,21].

We have also calculated the spin-dependent parts of $\bar{p}d$ cross section taking shadowing effects into account and compared them with the results obtained in Refs. [11,21]. In contrast to the authors of those papers we have made an attempt to take the double-scattering contribution

into account while calculating the spin-dependent parts of $\bar{p}d$ cross section. We conclude that polarized deuterium target can be used instead of the hydrogen target with similar or even higher efficiency. However, one can see fairly strong model dependence of the spin-dependent parts of the cross section. The Nijmegen model predicts higher polarization degree than the other models and this was the case for $\bar{p}p$ scattering too. Only experimental investigation of polarized $\bar{p}p$ or $\bar{p}d$ cross sections can show us what model is closer to the reality.

Acknowledgements

We are grateful to A.I. Milstein for valuable discussions. The work was supported in part by the Grant 14.740.11.0082 of Federal Program “Personnel of Innovational Russia”.

References

- [1] PAX Collaboration, Technical proposal for antiproton–proton scattering experiments with polarization, arXiv:hep-ex/0505054, 2005.
- [2] A.I. Milstein, V.M. Strakhovenko, Phys. Rev. E 72 (2005) 066503.
- [3] N.N. Nikolaev, F.F. Pavlov, Polarization buildup of stored protons and antiprotons: Filtext result and implications for pax at fair, arXiv:hep-ph/0601184, 2006.
- [4] A.I. Milstein, S.G. Salnikov, V.M. Strakhovenko, Nucl. Instr. Meth. Phys. Res. B 266 (2008) 3453.
- [5] P.L. Csonka, Nucl. Instr. Meth. 63 (1968) 247.
- [6] V.F. Dmitriev, A.I. Milstein, V.M. Strakhovenko, Nucl. Instr. Meth. Phys. Res. B 266 (2008) 1122.
- [7] V.F. Dmitriev, A.I. Milstein, S.G. Salnikov, Phys. Lett. B 690 (2010) 427.
- [8] PAX Collaboration, Measurement of the spin-dependence of the $\bar{p}p$ interaction at the AD-ring, arXiv:0904.2325, 2009.
- [9] V. Franco, R.J. Glauber, Phys. Rev. 142 (1966) 1195.
- [10] V. Franco, R.J. Glauber, Phys. Rev. 142 (1966) 1195.
- [11] Yu.N. Uzikov, J. Haidenbauer, Phys. Rev. C 79 (2009) 024617.
- [12] M.N. Platonova, V.I. Kukulín, Phys. Rev. C 81 (2010) 014004.
- [13] R. Timmermans, Th.A. Rijken, J.J. de Swart, Phys. Rev. C 50 (1994) 48.
- [14] M. Lacombe, et al., Phys. Rev. C 21 (1980) 861.
- [15] R. Bizzarri, et al., Nuovo Cimento A 22 (1974) 225.
- [16] T. Kalogeropoulos, G.S. Tzanakos, Phys. Rev. D 22 (1980) 2585.
- [17] R.D. Burrows, et al., Aust. J. Phys. 23 (1970) 819.
- [18] A.S. Carroll, et al., Phys. Rev. Lett. 32 (1974) 247.
- [19] R.P. Hamilton, T.P. Pun, R.D. Tripp, D.M. Lazarus, H. Nicholson, Phys. Rev. Lett. 44 (1980) 1182.
- [20] G. Bruge, et al., Phys. Rev. C 37 (1988) 1345.
- [21] Yu.N. Uzikov, J. Haidenbauer, J. Phys.: Conf. Ser. 295 (2011) 012087.